THE JOURNAL OF PHYSICAL CHEMISTRY B
A JOURNAL OF THE AMERICAN CHEMICAL SOCIETY

pubs.acs.org/JPCB Article

Single-Molecule Fluorescence Spectroscopy of Phase-Separated 10,12-Pentacosadynoic Acid Films

Published as part of The Journal of Physical Chemistry virtual special issue "W. E. Moerner Festschrift".

Alfred Yeboah, David Sowah-Kuma, Wei Bu, and Matthew F. Paige*

Cite This: *J. Phys. Chem. B* 2021, 125, 3953–3962 Read Online

ABSTRACT: Phase-separated monolayers of 10,12-pentacosadiynoic acid and perfluorotetradecanoic acid can be photopolymerized to produce micrometer-sized, fluorescent polydiacetylene fibers at the air−solid interface. The photopolymer fibers were not uniformly fluorescent but rather showed a series of fluorescent spots along their lengths. The spots exhibited the classic properties of single-molecule fluorescence emission, including diffraction-limited size and fluorescence intermittency ("on−off blinking"). We have analyzed the fluorescence blinking dynamics of these spots using a variety of single-molecule analysis approaches, including fluorescence intensity histograms, autocorrelation analysis, as well as cross-correlation analysis as a function of distance between individual transition dipole moments, and propose a simple physical model for the fiber structure based on the observed blinking dynamics, in which the polymer fibers contain numerous structural defects. The model was supported by grazing incidence X-ray diffraction measurements of the mixed monolayer films at the air−water interface, in which it was observed that the presence of perfluorocarbon in the mixed monolayers significantly inhibited the ability of the 10,12-pentacosadiynoic acid to polymerize.

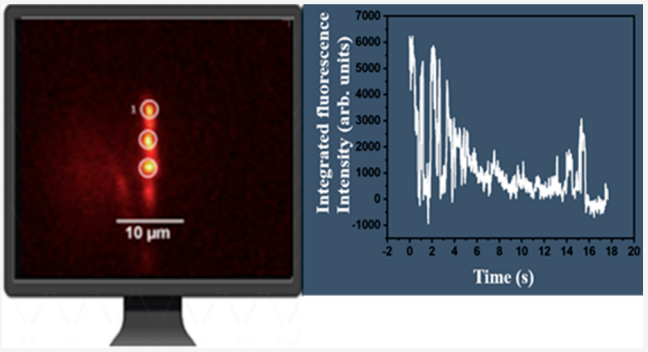

INTRODUCTION

Polydiacetylenes (PDAs) are a technologically useful class of conjugated polymers that have found use in a host of optical sensing applications.[1] For optical applications, their primary spectroscopic characteristic of interest is the ability to undergo a phase change between a blue, nonfluorescent form to a red, highly fluorescent form, with the conversion driven by a host of physical or chemical perturbations (i.e., mechanochromism, thermochromism, and targeted ligand−receptor binding). The color and fluorescence response of the polymer has been related to structural perturbations of the polymer chains resulting from the various binding or mechanical stressors described above,[1] and the optical spectroscopy of the different forms has been explored in depth.[2,3]

A wide range of different polydiacetylene monomer building blocks have been described in the literature, along with different polymerization strategies; however, a common approach to constructing polymer films is the photopolymerization of diacetylene (R−C≡C−C≡C−R′) monomers with UV or visible light. For thin films, the diacetylene monomers are often incorporated into surfactants, for example, 10,12-pentacosadiynoic acid (PCDA; $C_{24}H_{41}COOH$, structure included in Scheme 1), which are in turn formed into monolayers or bilayers using Langmuir monolayer or vesicle-based approaches, respectively. This allows for simple, tractable approaches to deposit photoresponsive films onto various solid substrates for further sensing applications (see Scindia et al., for example).[4]

Our research group's early interests in PDAs stem from attempts to pattern the photopolymer in a controlled fashion using phase-separation of monolayer films; in this approach, the PCDA monomer is mixed with a perfluorinated fatty acid, typically perfluorotetradecanoic acid (PF; $C_{13}F_{27}COOH$). The two components are immiscible because of the substantial difference in polarizabilities of the two types of surfactants, resulting in phase-separated domains of PCDA and PF at both the air−water and solid−air interfaces.[5−8] The process is illustrated in Scheme 1. By controlling the relative amounts of the two components in the mixed films, followed by photopolymerization with UV or visible light, some limited degree of control over the structure of the resulting polydiacetylene could be achieved. The photopolymer film

Received: February 1, 2021
Revised: March 20, 2021
Published: April 7, 2021

https://doi.org/10.1021/acs.jpcb.1c00951
J. Phys. Chem. B 2021, 125, 3953−3962

Scheme 1. Schematic Illustration of the Photopolymerization of a Phase-Separated Mixed PF−PCDA Surfactant Monolayer[a]

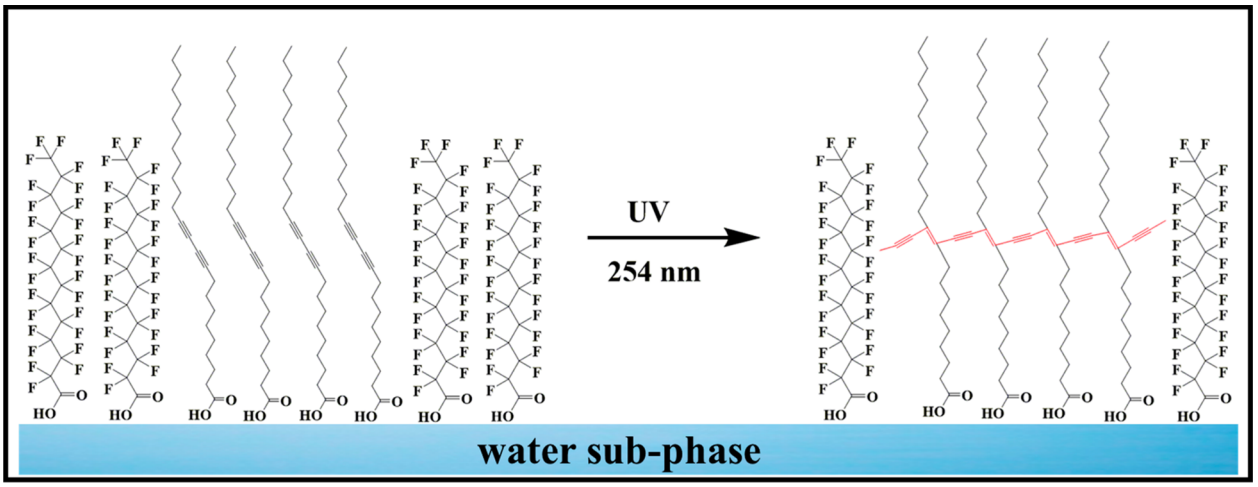

[a]Photopolymerization of PCDA proceeds via 1-4 addition of adjacent monomer units to produce the final conjugated polymer product. For simplicity, the polymer product is drawn as a monolayer, but bilayers and trilayers form under select conditions.

structures were complex and likely consisted of diacetylene bilayers that formed as a consequence of film buckling during the polymerization process. Similar multilayer structures (for example trilayers) are well-known in the polydiacetylene systems and have been reported by multiple authors under different circumstances,[9,10] including on solid substrates and at the air−water interface. Of particular interest to our research goals was the ability of the phase-separation approach to yield red fluorescent polymer fibers which were many hundreds of micrometers in length and exhibited (weakly) polarized emission.[8]

We have recently carried out a preliminary investigation of the structure of polymer fibers formed in a phase-separated film using a combination of fluorescence anisotropy imaging (FAIM) and defocused epifluorescence microscopy.[7] These imaging experiments revealed that a wide range of sizes and shapes of PDA fibers were formed throughout the film, but there was also considerable heterogeneity within each fiber, as revealed by large variations in fluorescence anisotropy. This was tentatively ascribed to each fiber consisting of bundles of polymer strands, with a wide variety of polymer strand orientations within the fiber. However, during this study we also made a serendipitous observation during defocused epifluorescence imaging experiments, in which for select fibers we observed "doughnut" emission patterns that were similar (but not identical) to those reported for individual transition dipoles (single molecules). Furthermore, conventional focused epifluorescence measurements revealed a population of the fibers that exhibited discrete "spots" running along their length, and these spots exhibited on−off fluorescence blinking that is typical of single-molecule emitters.

There is precedent for detection of emission of individual PDA molecules in the literature. Schott et al. have reported the detection of isolated red polydiacetylene chains in a 3BCMU crystal monomer matrix.[11] The authors have provided a detailed spectroscopic investigation of the emission from isolated red polymer chains, including emission spectra, fluorescence lifetimes, and temperature dependence of quantum yields. Further studies on isolated chains and affiliated color transitions, as well as recent reports of quantum-wire effects, are reviewed and discussed by the same research group elsewhere.[12,13]

Given our preliminary results and the work by Schott, we have carried out a more in-depth investigation of the fluorescence emission from the fibers formed using the phase-separation approach to verify that the on−off blinking spots detected previously were indeed individual emitters and to characterize their behavior within the larger fibers. We note that if these are indeed individual emitters then they are in an extremely different local environment from those reported by Schott et al., i.e., bound within a macromolecular polymer. Furthermore, energy transfer dynamics, including exciton trapping, resonant energy transfer, and other similar effects, are well-known in luminescent polymer systems and have been amenable to single-molecule studies; thus, we have also investigated the potential for energy transfer dynamics within this system. However, we also note that the fiber polymer structures studied in this study are complex, and this can reasonably be expected to have a significant impact on the spectroscopic output of the fibers. To help provide context to our single-molecule studies of the fibers, we have also characterized the molecular-level structures of the films at the air−water interface using synchrotron-based X-ray diffraction techniques and discuss the overall spectral properties of the system in the context of the film.

EXPERIMENTAL METHODS

Sample Preparation. PF and PCDA was purchased from Sigma-Aldrich. The solvents hexanes and tetrahydrofuran were HPLC-grade. All reagents were used as received. Microscope cover glass (VWR International) was cleaned with piranha solution, rinsed with absolute ethanol, and cleaned in a commercial plasma cleaner (Harrick Plasma) for ∼20 min at high power before use. Because of the light-sensitive nature of PCDA, films and solutions were prepared and stored in the dark whenever possible to minimize exposure to ambient room light.

Langmuir−Blodgett Film Preparation. Films were prepared using a Langmuir trough system (KSV-NIMA) equipped with a dipper for deposition. Ultrapure water (either Millipore or Barnstead) was used as a subphase. The water

https://doi.org/10.1021/acs.jpcb.1c00951
J. Phys. Chem. B 2021, 125, 3953−3962

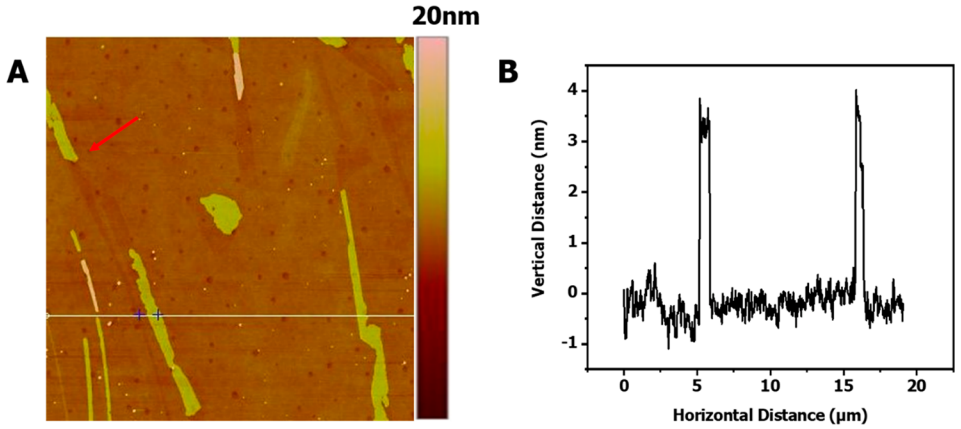

Figure 1. (A) AFM height mode images (20 μm × 20 μm) of a 7:1 mixed film after laser illumination (illumination time 20 s, with a solid-state laser of wavelength 532 nm on the film-covered substrate). (B) Cross section of the polymerized region of the film in (A).

surface was cleaned by suction before each measurement. Blank runs (compression of the clean water surface) showed no substantial change in surface pressure with compression. Stock solutions of PF and PCDA were prepared by dissolving the solid surfactant in a 9:1 volume ratio of hexanes/tetrahydrofuran to make final solutions each with concentration of 1×10^{-3} M. The PCDA solution was filtered with a syringe filter (0.45 μm) three times to remove traces of red polymer in the stock solution. The stock solutions were mixed to give a range of PF/PCDA mole ratios (7:1, 8:1, 9:1, and 10:1). A 100 μL aliquot of the surfactant solution was spread on the subphase surface, and the solvent was left to evaporate for at least 10 min before film compression. Films were compressed at a rate of ∼2.5 Å^2/molecule·minute until a deposition pressure of π = 15 mN/m was reached. After reaching the deposition pressure, the film was left to stabilize for ∼20 min before the cover glass substrate (oriented perpendicular to the subphase surface) was pulled upward through the water−air interface. The film was left to dry at room temperature in a clean environmental chamber before further measurements. Unless otherwise stated, measurements of deposited films were carried out on films with composition of 7:1, though results for other compositions were comparable with those reported in detail below.

Atomic Force Microscopy and Fluorescence Microscopy Measurements. Atomic force microscopy (AFM) measurements were performed in tapping mode in air using a Dimension Hybrid Nanoscope system (Bruker). Commercial Si_3N_4 AFM probes (Bruker), with spring constant of 10−30 N/m were used, and samples could be imaged repeatedly without detectable damage to the film. To observe the effect of photopolymerization, samples were imaged after exposing films to 532 nm laser light illumination in the fluorescence microscope described below.

Fluorescence images, time intensity trajectories, and emission spectra of the polymerized monolayer films were collected using a modified epifluorescence microscope with laser illumination that has been detailed described previously.[14] Briefly, the output from a solid-state laser (532 nm, Dragon Lasers) was focused onto the deposited films through a microscope objective lens (100×, 1.4 NA) to induce photopolymerization. Fluorescence emission from the polymerized film was collected back through the objective, passed through two long pass optical emission filters (540LP; Omega Filters) and directed onto the detector of choice. For images and time trajectories, the detector was an electron-multiplying CCD camera (IXon, Andor), and for fluorescence spectra, the detector was a miniature fiber-optic-based spectrometer (USB-2000, Ocean Optics). An illumination intensity of 0.2 kW/cm^2 was used for imaging experiments, with intensities determined by dividing the measured power at the microscope objective by the illumination area (spot diameter ∼ 10 μm).

Grazing Incidence X-ray Diffraction Measurements. Grazing incidence X-ray diffraction measurements (GIXD) measurements were performed on beamline 15-ID-C (NSF's ChemMatCARS) at the Advanced Photon Source (Argonne National Laboratories). Monolayers were prepared in a Langmuir trough equipped with a single barrier, and the trough was mounted on antivibration system and covered with a sealed enclosure equipped with X-ray transparent Kapton foil windows. The chamber was continuously purged with helium (molecular oxygen levels < 2%) to minimize X-ray induced film damage. After spreading the surfactant solution on the subphase with a Hamilton syringe, the solvent was left to evaporate, and the monolayer was compressed to the desired surface pressure (usually π = 15 mN/m). All experiments were conducted at room temperature. A Ge(111) steering crystal was used to direct monochromatic X-rays with an energy of 10.0 keV (λ = 1.24 Å) onto the liquid surface at a fixed incident angle. The diffracted X-ray beam was collected with a Pilatus 100 K X-ray detector (Dectris). Films were polymerized using a 254 nm UV lamp supported ∼10 cm away from the subphase surface. Diffraction intensity was measured as a function of both the in-plane (q_{xy}) and out-of-plane (q_z) scattering vectors. The experimental geometry has been illustrated and described in detail by Lin et al.[15]

RESULTS AND DISCUSSION

AFM imaging was used to characterize the morphology of the mixed, deposited films after laser illumination. A typical AFM image and cross section from a 7:1 mixed film after photopolymerization is shown in Figure 1. The film morphology consisted of a continuous flat (on the height scale of nanometers) matrix, mixed with a heterogeneous collection of fibers and patches that were elevated ∼3.0−4.0 nm above the flat matrix. The elevated regions typically sat in a slightly depressed region (0.5−1.0 nm), as highlighted by a red arrow in Figure 1. Fibers varied widely in length, width, and shape, but they most commonly had lengths in the range of ∼2−20 μm and widths of ∼1 μm. We have previously assigned

https://doi.org/10.1021/acs.jpcb.1c00951
J. Phys. Chem. B 2021, 125, 3953−3962

these structures to consist of bilayers of PDA (the elevated regions) surrounded by a matrix of PF (the flat matrix), with the depressed regions being bare glass. There was a slight tendency of the long axis of the fibers to point in a common direction, as a consequence of the mechanical force exerted by the Langmuir trough barriers on the film and by hydrodynamic flow of liquid off the glass substrates during postdeposition liquid draining.[8] These results are in excellent agreement with those we have reported previously.[6]

We have previously identified the elevated regions as being the photopolymer PDA, with the continuous flat matrix consisting primarily of PF and occasional regions of unpolymerized PCDA. This was further confirmed by the epifluorescence measurements (*vide infra*). The 7:1 mixtures were selected for further study but films with similar mixing ratios (8:1, 9:1, and 10:1) had comparable film morphology. Somewhat surprisingly, similar elevated strands could also be found on films that had not been illuminated with laser light. This implies that despite filtering the stock PCDA solutions trace quantities of polymer remain in the samples before deposition, that the samples can be polymerized by ambient light during the various stages of sample preparation, or both. We were unable to eliminate this effect despite various modifications to our sample preparation and handling protocols. Nonetheless, we were reproducibly able to prepare samples that contained either preformed PDA photopolymer or could be visibly photopolymerized in the epifluorescence microscope. Further fluorescence characterization of the samples using fluorescence microscopy is described in the following section.

Deposited films were imaged in the epifluorescence microscope using illumination intensities and EMCCD settings that were appropriate for single-molecule detection. Fluorescence images initially consisted of a dark, negligibly fluorescent background but after several seconds of illumination with the excitation laser, fluorescent fibers formed in the field of view, consistent with previous reports.[7] Images of several different fibers are shown in Figure 2. Fibers were heterogeneous in size and shape and could be found distributed across the entire glass substrate. The size, shape, and numbers of fibers found on the samples were qualitatively consistent with those found in the AFM imaging experiments above. Fluorescence intensity within each fiber was not uniform but rather consisted of "spots" of fluorescence running along its length, an effect which is explored in more detail below. Fiber fluorescence was visibly red through the microscope eyepiece. (***Caution**: Care should be taken when viewing samples through microscope eyepieces during laser illumination.*) To verify that the PDA formed in these experiments was indeed the red form of the polymer, emission spectra from individual fibers was measured on a fiber-optic spectrometer, with results from a typical fiber shown in Figure 2B. The emission spectrum for a fiber consisted of two broad peaks: a strong maximum centered at 560 nm and a weaker peak at 620 nm. This is the expected emission spectrum for red PDA,[6] verifying the formation of the red form of the polymer.

We turn now to the unusual distribution of fluorescence intensity within a red PDA fiber. As seen in Figure 2, the PDA fibers were not uniform in fluorescence but rather exhibited a series of well-defined spots that were distributed along their lengths. Each spot was typically ~300 nm in size, as determined by calibrating the EMCCD pixel size using a USAF test target, and while the separation between spots

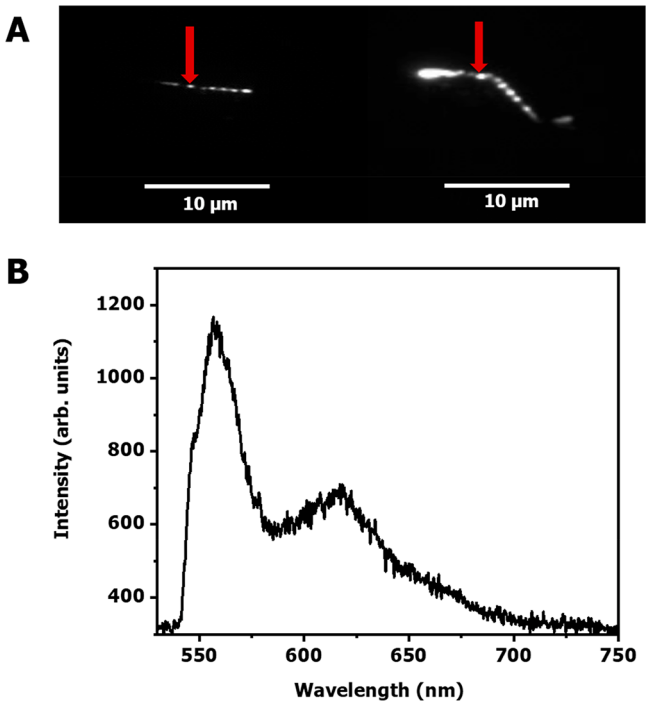

Figure 2. (A) Fluorescence microscopy images of fluorescent fibers measured in phase-separated 7:1 mixed films on a different part of a glass substrate (λ_{exc} = 532 nm and power of 0.4 mW at the sample focal plane). The red arrow indicates a fluorescent spot as detailed in the body text. (B) Corresponding fluorescence emission spectrum of a 7:1 mixed monolayer on a glass substrate after photopolymerization with a 532 nm, 0.4 mW laser for ~1 min.

varied from spot-to-spot and from fiber-to-fiber, the center-to-center distance between spots was estimated to be on the order of 2−3 μm (see Figure S1 for a cross-sectional analysis). Of particular interest was that the emission of individual spots was not continuous but rather exhibited on−off blinking, switching between a highly fluorescent state and a minimally fluorescent state (see Movie S1). Fluorescence−time trajectories of two different spots on the same fiber have been collected and are shown in Figure 3B. The time trajectories for the spots showed multiple single stepwise changes in fluorescence intensity, before ultimately irreversibly photobleaching (typically after ~20 s). In addition to the characteristic on−off blinking, some of the trajectories also exhibited a slowly decreasing background fluorescence. Two spots have been analyzed in Figure 3A (the red box is a 3 pixel × 3 pixel region of interest that contains the spot) to highlight the fluorescence fluctuation and photobleaching event. For time trajectories, a simple background subtraction using a region-of-interest that was well away from a fluorescent fiber was first carried out, but it was found that for many trajectories there was often still a slowly decreasing background that was not removed using this process. We have seen this effect previously[7] and believe the additional background comes from out of focus PDA (one layer of the bilayer; either red or blue PDA) which is present in the excitation volume but out of the immediate focal plane, and this component is slowly photobleaching during the experiment. To correct for this, a second-order function ($I(t) = At^2 + Bt + C$, where I is integrated fluorescence intensity, t is time, and A, B, and C are empirical fitting constants) was subtracted from the data to account for the time varying

https://doi.org/10.1021/acs.jpcb.1c00951
J. Phys. Chem. B 2021, 125, 3953−3962

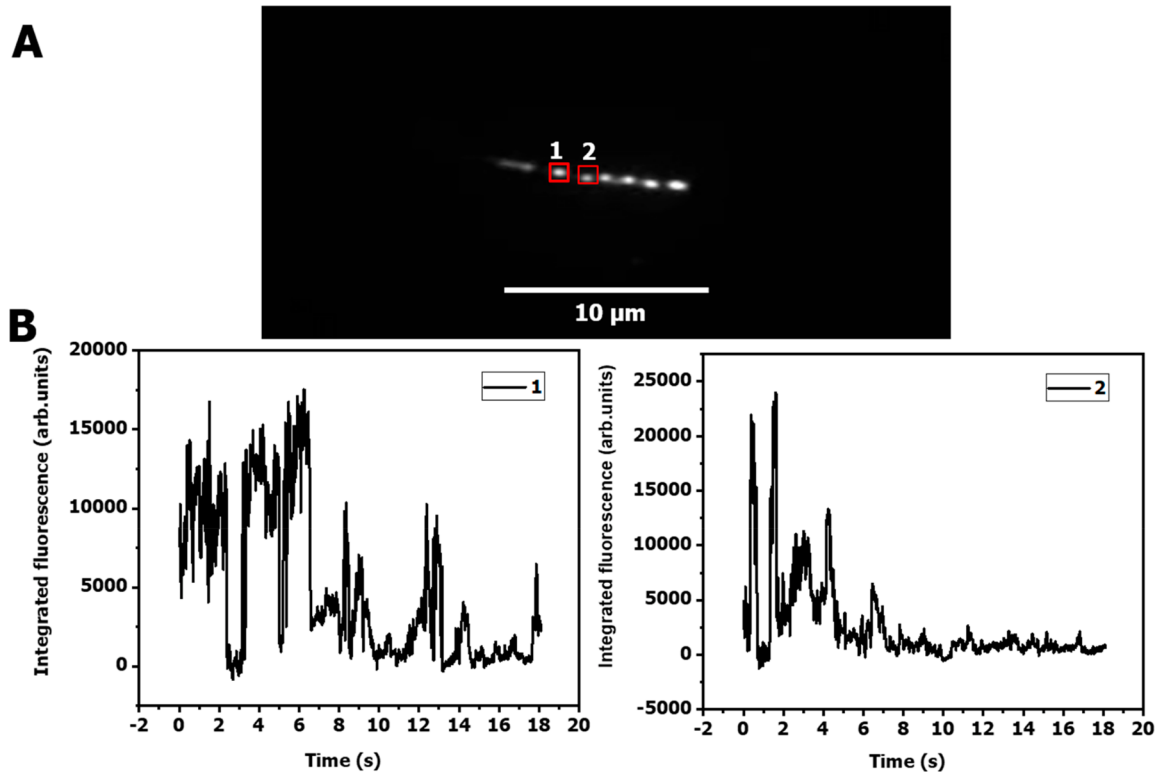

Figure 3. (A) Fluorescence images of short fibers measured in phase-separated 7:1 films on a glass substrate (λ_{exc} = 532 nm). (B) Fluorescence time trajectories of the individual spots 1 and 2 on the fiber.

fluorescence background intensity, and these background-corrected trajectories were used for further analysis.

The combination of on−off blinking dynamics along with the diffraction-limited size of the spots is consistent with single-molecule behavior, suggesting that emission from the spots is from discrete PDA transition dipoles within the larger fibers. To further support this, additional analysis has been carried out on the time trajectories. Figure 4 shows representative normalized autocorrelation curves ($g^2(\tau) = \langle I(t)\cdot I(t+\tau)\rangle/\langle I(t)\rangle^2$) for time trajectories measured at two different laser illumination intensities, along with a single-exponential decay function overlaid on the autocorrelation curve, provided as a guide to the eye. At lower illumination intensities, the on−off blinking effects were readily discernible in the autocorrelation curves, with blinking manifesting as features at the characteristic time scale of the blinking, as expected.[16,17] Autocorrelation curves were different for each spot's trajectory, with each spot exhibiting its own unique blinking dynamics, though features were most commonly observed at τ < 5 s, consistent with faster "flickering" of fluorescence intensity.

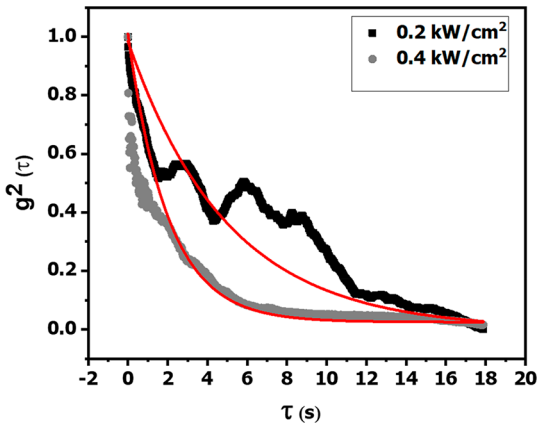

Figure 4. Normalized intensity time correlation functions for two laser excitation intensities for a single emission transition dipole of PDA. Black line, sample excited with 0.2 kW/cm^2 laser intensity; gray line, sample excited with 0.4 kW/cm^2 excitation laser intensity. The red overlay lines are single-exponential curves included as a guide to the eye.

As a simple assessment of the rate of correlation decrease, data were overlaid with single-exponential decays, a function that is consistent with single-molecule behavior that follows two-state kinetics.[18] We note that the overlays are not intended as quantitative fits of the data and that the peaks and valleys in the curves which are characteristic of the on−off blinking are not expected to follow this function. At higher illumination intensities, correlation functions decayed more rapidly, indicating that shorter "on" times dominate and the blinking-attributed features that were readily detectable at lower intensities were difficult to discern, presumably because the blinking rate becomes fast in comparison to our integration interval (100 ms). The illumination intensity dependence on fluorescence emission in single-molecule and CdSe quantum dot systems is well-known.[19] While we have not attempted to carry out a detailed illumination intensity study here, we note that a simple doubling of the illumination intensity leads to an approximate doubling of the correlation decay rate, suggesting that excited state emission and relaxation in this system might be described by a relatively simple, light-driven kinetic scheme as opposed to some of the more complex models (e.g., five states, including T_n where n > 1 excited triplet states) that have been needed to describe blinking behavior in small organic dye

https://doi.org/10.1021/acs.jpcb.1c00951
J. Phys. Chem. B 2021, 125, 3953−3962

systems.[20,21] As a simple control experiment, we also measured samples that had been coated with a thin layer of poly(methyl methacrylate) to minimize oxygen access to the fluorophores. There was no gross difference in on−off blinking behavior observed with the polymer oxygen barrier in place, suggesting a minimal role for atmospheric oxygen (i.e., triplet state quenching) in the blinking. While we do not yet have sufficiently detailed information to determine the underlying mechanism of blinking in this system, it is clearly a light-driven process. We had originally speculated that if the spots were transition dipoles associated with single PDA polymer strands then a possible source of blinking in the system might be energy transfer between adjacent PDA strands. The spatial separation between spots (typically several microns as noted above) is significantly greater than that for efficient Dexter or Förster energy transfer, but we nonetheless attempted to assess any correlation between blinking events on spots within the same fiber by calculating intensity cross-correlation values as a function of separation between spots. While the analysis suffered from unexpectedly high cross-correlation values, likely because of issues with imperfect background correction, there was no discernible trend in cross-correlation values as a function of spot separation, suggesting that interfiber energy transfer is not a contributing factor in the blinking.

We have also generated fluorescence intensity histograms from the individual "on" events pooled from time trajectories of ∼150 individual blinking spots collected from multiple PDA fibers and report results in Figure 5. For intensity histograms,

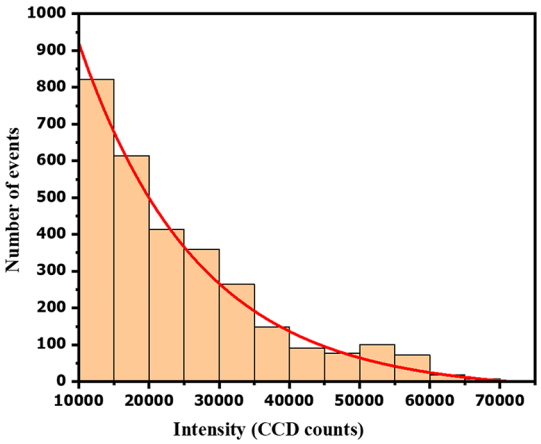

Figure 5. Histogram and single exponential fit of fluorescence intensity distribution for fluorescence time trajectories. The red line is a single-exponential decay function provided as a guide to the eye. Only fluorescence events with an intensity of $>10^4$ counts were recorded.

"on" events with intensities below a threshold of $<10^4$ counts were deemed to be unacceptably close to background and were excluded from the analysis; all other events were included. Fluorescence intensity distributions for individual fluorophores with a single population are expected to follow Poisson statistics and thus should follow a simple single-exponential decay.[18] As seen in Figure 5, the fluorescence intensity histogram was fit well by a single-exponential function, which is consistent with a single population of emitters, and there was no indication of different subpopulations, suggesting that despite the highly heterogeneous nature of the PDA fibers, the individual emitting units within each fiber are in broadly similar local environments and emit through similar decay pathways.

We consider now the underlying polymer fiber structure and how this relates to the fluorescence emission that is observed. The cumulative evidence described above, including the fluorescence blinking dynamics, autocorrelation analysis, and intensity distributions, indicate we are detecting individual emission transition dipole moments of PDA within the larger polymer fibers and that the transition dipole moments are both physically and electronically separated, despite being part of the same larger fiber structure. This suggests a model in which fibers are bilayers comprised of highly fragmented bundles of PDA polymer strands, with each polymer strand serving as an independent emission dipole moment. Background emission comes from fluorescence contributions from the out-of-focus layer. We know that there is significant fiber-to-fiber heterogeneity.[7] In some cases, fibers likely contain a large fraction of the nonemissive blue PDA strands or physical defects such as kinks or folds in the polymer strands, which disrupt the conjugation of the polymer and render substantial regions of the fiber nonfluorescent. For these fibers, we detect only occasional, discrete emission transition dipoles from red polymer strands. In other fibers, where there is significantly less blue PDA and/or minimal physical defects, the fibers give off more uniform red PDA emission, and individual transition dipoles cannot be detected. A simple 2D illustration of this is provided in Scheme 2, with fragments of PDA depicted as simple "dimers" of PCDA in the first layer and bilayers drawn with an assumption of tail-to-tail orientation. While this proposed model seems plausible, additional characterization of film structure is clearly needed to support or refute this, and we have thus turned to GIXD measurements of the 7:1 mixed films directly at the air−water interface.

Monolayers of PCDA and the resulting photopolymers films formed at the air−water interface have been studied extensively in the literature using synchrotron-based diffraction methods, with measurements indicating that the precise molecular structure of the films are highly dependent upon subphase, compression, and X-ray irradiation conditions.[9,10,22] Under arguably the most in-depth studied conditions,[9] Lifshitz compressed PCDA monolayers that are exposed to prolonged irradiation with UV light evolve through a series of complex structures, starting from the PCDA monomer phase (hexagonal order with normally oriented carboxyl-terminated chains and tilted alkyl chains) and ending with a trilayer red PDA structure (vertically oriented alkyl chains and two underlying sublayers from methyl-terminated chains and carboxyl-terminated chains), with variants of the blue PDA phase appearing as a function of irradiation time. However, variations on these results can be found elsewhere, likely because of differences in film preparation and irradiation. Garcia-Espejo et al.[23] have investigated mixtures of PCDA with a hemicyanine dye derivative and reported an orthorhombic molecular packing arrangement in which PCDA monomers are arranged in alternating rows with the hemicyanine dye (a miscible system), but the ability of the monomer to undergo polymerization was unimpeded. More broadly, the authors observed that the photopolymer product formed by illumination was the red PDA, with no detectable blue polymer in the mixture.

GIXD measurements of pure and mixed monolayer films for the PF−PCDA system, before and after photopolymerization with UV light are shown in Figure 6. For the pure PF

https://doi.org/10.1021/acs.jpcb.1c00951
J. Phys. Chem. B 2021, 125, 3953−3962

Scheme 2. Schematic Illustration of Postulated Fiber Structure at the Air−Solid Interface[a]

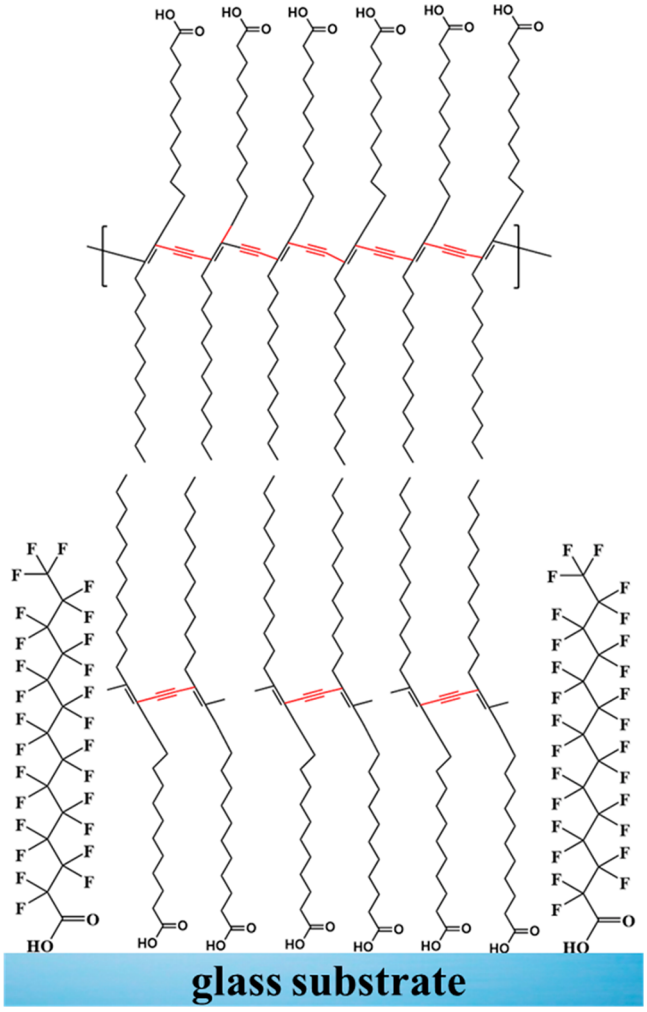

[a]Fibers consist of PCDA bilayers surrounded by PF, with considerable fragmentation of individual PCDA strands within each fiber.

monolayer (Figure 6 A), diffraction patterns consisted of a single, sharp Bragg peak at q_{xy} = 1.26 Å^{-1} with out-of-plane scattering vector at q_z = 0 Å^{-1}, which was indexed as a hexagonal lattice ($a = b$ = 5.77 Å, γ = 120°) and a unit cell area per chain of 28.8 Å. Bragg rods showed a nearest-neighbor (NN) tilt angle of zero, corresponding to PF molecules aligned normal to the subphase surface. These results agree well with previous literature reports from our group and others,[24−26] and indicate a highly crystalline monolayer at the air−water interface. The diffraction pattern for pure PCDA monolayers was more complex (Figure 6 B), and consisted of three strong diffraction peaks, including two in-plane peaks at q_{xy} = 1.30 and 1.37 Å^{-1}, as well as a broad, diagonally oriented out-of-plane peak at ca. q_{xy} = 1.20 Å^{-1}, q_z = 1.10 Å^{-1}. The peaks at q_{xy} = 1.37 Å^{-1} and q_z = 1.10 Å^{-1} were assigned to the PCDA monomer, packed with hydrophilic carboxyl-terminated alkyl chains perpendicular to the surface normal, and hydrophobic methyl-terminated alkyl chaines tilted toward the NN, consistent with trilayer formation reported by Lifshitz.[9] The comparatively weak in-plane diffraction peak at q_{xy} = 1.30 Å^{-1} is assigned to the blue polymer phase ($(02)_{B1}$ using the Miller indices and notation from Lifshitz), indicating that under the film preparation conditions used here, the "pure" monomer films contained traces of blue PDA. This agrees with the observations of trace amounts of polymer in the fluorescence measurements prior to illumination, though we cannot rule out the possibility that the X-ray beam is inducing some polymerization during the GIXD measurements (typical irradiation time per diffraction pattern was ∼30 min).

GIXD patterns for the mixed monolayer before UV illumination are shown in Figure 6C. Surprisingly, the only detectable reflection was that associated with the PF monolayer; there were no discernible reflections associated with the PCDA monolayer or from trace amounts of photopolymer product. Phase-separated monolayers with two components typically yield diffraction patterns which are simple linear combinations of the two individual monolayers,[27] and that is clearly not the case with this system. While this result might be due to simple dilution and signal-to-noise issue, with the relatively small amount of PCDA in the mixed film giving comparatively weak signal that falls below the limit of detection of the measurement, this seems unlikely; careful inspection of the data gave no indication of a meaningful signal for even the strongest q_z = 1.10 Å^{-1} monomer reflection. This suggests that the presence of PF perturbs the packing of the PCDA monomer and hinders its ability to form ordered, crystalline films such that any diffraction signal becomes immeasurably small. Precisely why this happens remains unclear, but we note that PCDA polymerization is a topochemical process, requiring precise spatial organization between monomers and disrupting this packing can significantly impact the ability to polymerize. This might also explain the lack of trace polymer in the mixed films, though again, this might be convoluted with signal-to-noise and detection limit issues. We note that Garcia-Espejo et al.[23] did not observe any significant impediment to polymerization in their mixed system, indicating the effect is specific to the perfluorocarbon-containing monolayers.

Illumination of the mixed film with UV light resulted in the slow appearance of new reflections associated with formation of photopolymer (Figure 6D). In addition to the always-present PF reflection, new in-plane reflections (q_{xy} = 1.45 and 1.60 Å^{-1}) grew in over the time course of approximately 0.5 h. The diffraction pattern is consistent with an orthorhombic cell (a = 5.2 Å, b = 7.8 Å, and a unit cell area per chain of of 20.4 Å^2). The peaks correspond to the $(11)_{R2}$ and $(02)_{R2}$ reflections for the red polymer phase using Lifshitz's model, albeit with no molecular tilt with respect to the subphase surface. These results indicate the gradual formation of small quantities of the red polymer at the air−water interface, with alkyl tails normal to the surface; thus, the conjugation length of the polymer running approximately parallel to the subphase surface. Intriguingly, control experiments of pure PCDA films alone using the same illumination conditions resulted in near instantaneous (<1 s) formation of a visibly red polymer film across the entire monolayer and enormous scattering signals. Clearly, the presence of PF in the monolayer, even in films where there is still a large quantity of monomer available to be cross-linked, significantly impedes the efficiency of the PCDA polymerization process. This is consistent with the GIXD measurements on the nonilluminated, mixed films where there was no detectable reflections attributed to the PCDA monolayer. Perfluorinated alkanes are rigid and inflexible in comparison with simple alkanes, and their monolayers are rigid and incompressible.[25,26] We postulate that the PF forms a

https://doi.org/10.1021/acs.jpcb.1c00951
J. Phys. Chem. B 2021, 125, 3953−3962

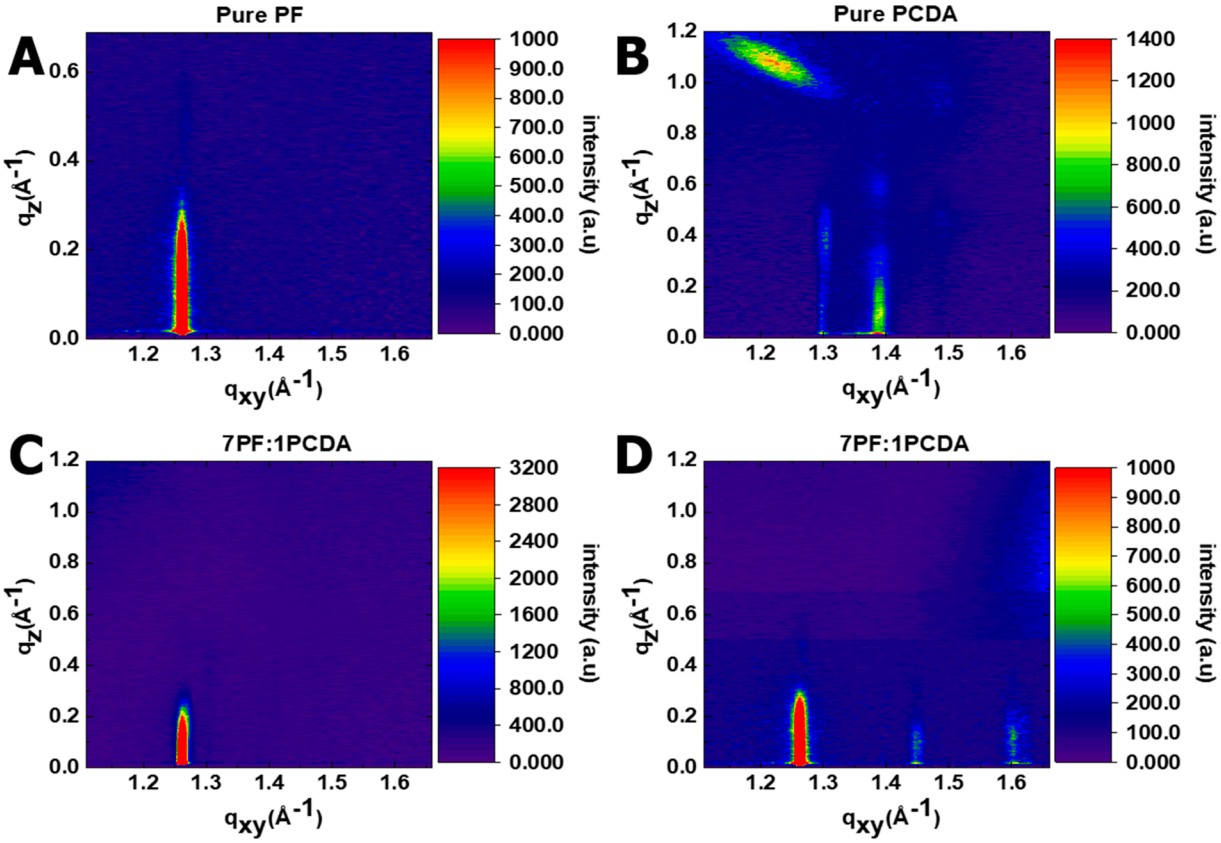

Figure 6. Contour plots showing diffraction intensity along q_z as a function of q_{xy} at π = 15 mN/m for (A) pure PF; (B) pure PCDA; (C) 7:1 film before irradiation; and (D) 7:1 film after 30 min of UV irradiation.

rigid, inflexible "matrix" and that the PCDA monomers are forced to adopt a spatial orientation within this rigid matrix that is poorly suited for polymerization.

We turn now to the implications of the GIXD results on the fluorescence properties of the fibers. The presence of PF in the mixed films clearly impedes the polymerization process, likely by disrupting the spatial organization of the PCDA monolayer. Only a small fraction of the total PCDA present has the correct topochemical alignment to polymerize, ultimately yielding very small quantities of "successfully" polymerized red PDA. These regions appear as the heterogeneous collection of red PCDA fibers and aggregates in the fluorescence images. Furthermore, the fluorescence measurements suggest that even these fibers are highly defect-rich and are effectively short bundles of independent polymer strands that behave like discrete emitters. A key interest in PCDAs is using their color response for film-based bio- and chemical-sensing applications. For these applications, production of small polymer fibers (or even individual polymer strands) that are defect-free would allow for large optical signal changes to be measured from very small regions of samples. This would enable high-sensitivity applications, for example, microarray-type sensors. Ultimately, if individual, defect-free individual polymer strands could be patterned, then spatial separations between sensing elements that are smaller can be achieved by photolithography. Future investigations on this system will be directed at tailoring mechanical properties of the PF matrix to further control and potentially minimize defects in the photopolymer strands, with an end goal of clarifying the role of matrix rigidity and defects on the optical properties of the photopolymer. An additional approach of interest in this regard is the use of solvent vapor annealing[28,29] to "relax" mechanically stressed polymer strands postillumination, to assess whether this is an important factor in controlling optical properties. Similar approaches have been used to anneal a variety of mechanically strained polymers, including misfolded poly(2-methoxy-5-(2′-ethylhexyloxy)-1,4-phenylene-vinylene) strands.[30] For the latter systems, solvent vapor annealing enabled single-molecule fluorescence-based tracking of the defect removal in the polymer, and similar effects might prove insightful for the single-emitter PDA system studied here.

CONCLUSIONS

This work describes the formation of micrometer-sized fibers of the photopolymer PDA in phase-separated monolayer films that are enriched in a perfluorinated surfactant and the characterization of these fibers using a combination of fluorescence imaging and liquid X-ray scattering techniques. Previous studies on these systems identified the photopolymer fibers formed in the monolayer films as being heterogeneous in both structure and fluorescence emission characteristics, and in this work, we have unambiguously detected single-molecule emission from different regions of the polymer fibers. Intermittent (on−off) fluorescence from multiple discrete emitters was observed along the lengths of fibers, though there was no correlation between blinking indicating a lack of electronic energy transfer between emissive units. To our knowledge, this is the first ever report of single-molecule emission of PDA detected in macroscopic polymer fibers. Surface-sensitive X-ray diffraction measurements on monolayers at the air−water interface both before and after photoillumination revealed that the presence of the perfluor-

https://doi.org/10.1021/acs.jpcb.1c00951
J. Phys. Chem. B 2021, 125, 3953−3962

ocarbon in the monolayer inhibits polymerization, likely by disrupting the precise film structure required for topochemical process. We postulate that this disruption, likely exacerbated by highly rigid nature of perfluorcarbon monolayers, also disrupts the structure within each fiber, and thus the single-molecule emission from the fibers is due to discrete polymer strands within a defect-rich larger fiber structure.

■ ASSOCIATED CONTENT

Supporting Information

The Supporting Information is available free of charge at https://pubs.acs.org/doi/10.1021/acs.jpcb.1c00951.

Fluorescence image of a fiber measured in a 7:1 film on a glass substrate containing four single emitters, corresponding intensity against distance for each spot on the fiber (PDF)

Movie S1: On−off blinking of 7:1 mixed film (AVI)

■ AUTHOR INFORMATION

Corresponding Author

Matthew F. Paige − *Department of Chemistry, University of Saskatchewan, Saskatoon, Saskatchewan S7N 5C9, Canada;* orcid.org/0000-0002-5552-8123; Email: matthew.paige@usask.ca

Authors

Alfred Yeboah − *Department of Chemistry, University of Saskatchewan, Saskatoon, Saskatchewan S7N 5C9, Canada*

David Sowah-Kuma − *Department of Chemistry, University of Saskatchewan, Saskatoon, Saskatchewan S7N 5C9, Canada*

Wei Bu − *NSF's ChemMatCARS, The University of Chicago, Chicago, Illinois 60637, United States;* orcid.org/0000-0002-9996-3733

Complete contact information is available at: https://pubs.acs.org/10.1021/acs.jpcb.1c00951

Notes

The authors declare no competing financial interest.

■ ACKNOWLEDGMENTS

Financial support for this work has been provided by the Natural Sciences and Engineering Research Council, the Canadian Foundation for Innovation, and the University of Saskatchewan. NSF's ChemMatCARS Sector 15 is supported by the Divisions of Chemistry (CHE) and Materials Research (DMR), National Science Foundation, under grant number NSF/CHE-1834750. Use of the Advanced Photon Source, an Office of Science User Facility operated for the U.S. Department of Energy (DOE) Office of Science by Argonne National Laboratory, was supported by the U.S. DOE under Contract No. DE-AC02-06CH11357.

■ REFERENCES

(1) Carpick, R. W.; Sasaki, D. Y.; Marcus, M. S.; Eriksson, M. A.; Burns, A. R. Polydiacetylene Films: A Review of Recent Investigations into Chromogenic Transitions and Nanomechanical Properties. *J. Phys.: Condens. Matter* **2004**, *16* (23), R679−R697.

(2) Schott, M. The Colors of Polydiacetylenes: A Commentary. *J. Phys. Chem. B* **2006**, *110* (32), 15864−15868.

(3) Carpick, R. W.; Mayer, T. M.; Sasaki, D. Y.; Burns, A. R. Spectroscopic Ellipsometry and Fluorescence Study of Thermochromism in an Ultrathin Poly (Diacetylene) Film : Reversibility and Transition Kinetics. *Langmuir* **2000**, *16* (10), 4639−4647.

(4) Scindia, Y.; Silbert, L.; Volinsky, R.; Kolusheva, S.; Jelinek, R. Colorimetric Detection and Fingerprinting of Bacteria by Glass-Supported Lipid/Polydiacetylene Films. *Langmuir* **2007**, *23* (8), 4682−4687.

(5) Araghi, H. Y.; Paige, M. F. The Effect of Perfluorotetradecanoic Acid on the Structure of Photopolymerized 10,12-Pentacosadiynoic Acid Films at the Air−Water Interface. *Can. J. Chem.* **2013**, *91* (11), 1130−1138.

(6) Younesi Araghi, H.; Paige, M. F. Deposition and Photopolymerization of Phase-Separated Perfluorotetradecanoic Acid-10, 12-Pentacosadiynoic Acid Langmuir Blodgett Monolayer Films. *Langmuir* **2011**, *27* (17), 10657−10665.

(7) Soleimaninejad, H.; Ghiggino, K. P.; Smith, T. A.; Paige, M. F. Fluorescence Anisotropy Imaging of a Polydiacetylene Photopolymer Film. *Can. J. Chem.* **2019**, *97* (6), 422−429.

(8) Araghi, H. Y.; Giri, N. K.; Paige, M. F. Polarized Fluorescence Microscopy Analysis Of Patterned, Polymerized Perfluorotetradecanoic Acid−Pentacosadiynoic Acid Thin Films. *Spectrochim. Acta, Part A* **2014**, *129*, 339−344.

(9) Lifshitz, Y.; Golan, Y.; Konovalov, O.; Berman, A. Structural Transitions in Polydiacetylene Langmuir Films. *Langmuir* **2009**, *25* (8), 4469−4477.

(10) Day, D.; Lando, J. B. Structure Determination of a Poly(Diacetylene) Monolayer. *Macromolecules* **1980**, *13* (6), 1483−1487.

(11) Lécuiller, R.; Berrehar, J.; Lapersonne-Meyer, C.; Schott, M.; Ganière, J.-D. Fluorescence Quantum Yield and Lifetime of 'Red' Polydiacetylene Chains Isolated in Their Crystalline Monomer Matrix. *Chem. Phys. Lett.* **1999**, *314*, 255−260.

(12) Spagnoli, S.; Berréhar, J.; Lapersonnemeyer, C.; Schott, M. Polydiacetylene Chains Diluted in Their Single crystal Monomer Matrix. *J. Chem. Phys.* **1994**, *100* (9), 6195−6202.

(13) Schott, M. Isolated Polydiacetylene Chains Dispersed in Their Monomer Crystal : One-Dimensional Organic Quantum Wires. *Synth. Met.* **2003**, *139*, 739−742.

(14) Bagh, S.; Paige, M. F. Construction and Application of a Single-Molecule Fluorescence Microscope. *Can. J. Chem.* **2005**, *83* (5), 435−442.

(15) Lin, B.; Meron, M.; Gebhardt, J.; Graber, T.; Schlossman, M. L.; Viccaro, P. The liquid Surface/interface Spectrometer at ChemMatCARS Synchrotron Facility at the Advanced Photon Source. *Phys. B* **2003**, *336* (1−2), 75−80.

(16) Suzuki, K.; Habuchi, S.; Vacha, M. Blinking of Single Dye Molecules in a Polymer Matrix Is Correlated with Free Volume in Polymers. *Chem. Phys. Lett.* **2011**, *505* (4−6), 157−160.

(17) Messin, G.; Hermier, J. P.; Giacobino, E.; Desbiolles, P.; Dahan, M. Bunching and Antibunching in the Fluorescence of Semiconductor Nanocrystals. *Opt. Lett.* **2001**, *26* (23), 1891−1893.

(18) Moerner, W. E.; Kador, L. Optical Detection and Spectroscopy of Single Molecules in a Solid. *Phys. Rev. Lett.* **1989**, *62* (21), 2535−2538.

(19) Shimizu, K. T.; Neuhauser, R. G.; Leatherdale, C. A.; Empedocles, S. A.; Woo, W. K.; Bawendi, M. G. Blinking Statistics in Single Semiconductor Nanocrystal Quantum Dots. *Phys. Rev. B: Condens. Matter Mater. Phys.* **2001**, *63*, 1−5.

(20) Eggeling, C.; Widengren, J.; Rigler, R.; Seidel, C. A. M. Photobleaching of Fluorescent Dyes under Conditions Used for Single-Molecule Detection: Evidence of Two-Step Photolysis. *Anal. Chem.* **1998**, *70* (13), 2651−2659.

(21) Gensch, T.; Böhmer, M.; Aramendía, P. F. Single Molecule Blinking and Photobleaching Separated by Wide-Field Fluorescence Microscopy. *J. Phys. Chem. A* **2005**, *109* (30), 6652−6658.

(22) Gourier, C.; Alba, M.; Braslau, A.; Daillant, J.; Goldmann, M.; Knobler, C. M.; Rieutord, F.; Zalczer, G. Structure and Elastic Properties of 10−12 Pentacosadiyonic Acid Langmuir Films. *Langmuir* **2001**, *17* (21), 6496−6505.

(23) García-Espejo, G.; Pérez-Morales, M.; Goldmann, M.; Martín-Romero, M. T.; Giner-Casares, J. J.; Camacho, L. Organization and

Structure of Mixed Langmuir Films Composed of Polydiacetylene and Hemicyanine. *J. Colloid Interface Sci.* **2017**, *508*, 583−590.
(24) Sowah-Kuma, D.; Fransishyn, K. M.; Cayabyab, C.; Martynowycz, M. W.; Kuzmenko, I.; Paige, M. F. Molecular-Level Structure and Packing in Phase-Separated Arachidic Acid-Perfluorotetradecanoic Acid Monolayer Films. *Langmuir* **2018**, *34* (36), 10673−10683.
(25) Barton, S. W.; Goudot, A.; Bouloussa, O.; Rondelez, F.; Lin, B.; Novak, F.; Acero, A.; Rice, S. A. Structural Transitions in a Monolayer of Fluorinated Amphiphile Molecules. *J. Chem. Phys.* **1992**, *96* (2), 1343−1351.
(26) Jacquemain, D.; Wolf, S. G.; Leveiller, F.; Lahav, M.; Leiserowitz, L.; Deutsch, M.; Kjaer, K.; Als-Nielsen, J. Dynamics of Two-Dimensional Self-Aggregation: Pressure and PH-Induced Structural Changes in a Fluorocarbon Amphiphile at Liquid-Air Interfaces. An X-Ray Synchrotron Study. *J. Am. Chem. Soc.* **1990**, *112* (21), 7724−7736.
(27) Takiue, T.; Vollhardt, D. Miscibility of Alkanol and Fluoroalkanol in Langmuir Film at the Air/Water Interface. *Colloids Surf., A* **2002**, *198*−*200*, 797−804.
(28) Sinturel, C.; Vayer, M.; Morris, M.; Hillmyer, M. A. Solvent Vapor Annealing of Block Polymer Thin Films. *Macromolecules* **2013**, *46* (14), 5399−5415.
(29) Jin, C.; Olsen, B. C.; Luber, E. J.; Buriak, J. M. Nanopatterning via Solvent Vapor Annealing of Block Copolymer Thin Films. *Chem. Mater.* **2017**, *29* (1), 176−188.
(30) Vogelsang, J.; Brazard, J.; Adachi, T.; Bolinger, J. C.; Barbara, P. F. Watching the Annealing Process One Polymer Chain at a Time. *Angew. Chem., Int. Ed.* **2011**, *50* (10), 2257−2261.

https://doi.org/10.1021/acs.jpcb.1c00951
J. Phys. Chem. B 2021, 125, 3953−3962